Whole Angle Mode for Low Q-factor Vibratory Gyroscopes

V V Chikovani[1,3], V M Azarskov[1] and S V Golovach[2]

[1,2] Aerospace control systems Department, National Aviation University, 1 Liubomyra Huzara ave., Kyiv 03058, Ukraine
[2] PJSC "Elmiz", 9 Borispolskaya str., Kyiv 02099, Ukraine

[3] E-mail: v_chikovani@ukr.net

Abstract. This paper considers whole angle mode operation for vibratory gyroscopes based on the low Q-factor resonators. It has the main disadvantage consisting in a large dead zone that makes them unable to measure angles at small angle rate. So, many MEMS and low-cost non-MEMS CVGs have sufficiently large damping mismatch to operate in whole angle mode. It is because whole angle mode is very sensitive to a resonator imperfection. The presence of an even small damping mismatch results in a non-sensitivity to small angle rate, that is to so-called dead zone. Moreover, out of dead zone there appears periodic error when measuring angle of rotation. This fact prevents creation of a dual mode and a triple mode low cost CVGs. This paper discusses the main errors resulting in dead zone. Virtual rotation of a standing wave with an angle rate much more than dead zone threshold is used to overcome it. Correction model of a periodic error caused by case-oriented drift is considered to reduce angle measurement error.

1. Introduction

Coriolis Vibratory gyro (CVG) is the most widespread of the recent gyroscopic technology in the world market. This technology has filled the world market in a fairly short time, primarily due to its micro-miniature version based on a microelectromechanical system (MEMS). MEMS CVGs technology is suitable to mass production and, hence, can be low-cost. They usually do not undergo a mass balancing procedure to reduce damping mismatch (Q-factor mismatch), but electrical balancing is used to reduces frequency mismatch staying in low-cost grade gyroscopes. As to non-MEMS (bulk) low-cost CVGs the mass balancing procedure on fourth harmonic of Fourier decomposition are usually made to reduce frequency mismatch, but it is not sufficient to reduce damping mismatch. To reduce damping mismatch all four harmonics of a mass imbalance should be made, which is a time-consuming and expensive procedure. Thus, MEMS and low-cost non-MEMS CVGs have sufficiently large damping mismatch to operate in whole angle mode. It is because whole angle mode is very sensitive to a resonator imperfection. The presence of an even small damping mismatch results in a non-sensitivity to small angle rate, that is to so-called dead zone [1]. Moreover, out of dead zone there appears periodic error when measuring angle of rotation. The amplitude of this periodic error is proportional a damping mismatch with a small addition from the residual value of frequency mismatch. This fact prevents creation of a dual mode [2] and a triple mode [3] low cost CVGs with automatic switching from one mode to another using advantages of each mode to minimize measurement errors.

There are two well-known, rate and rate-integrating, modes of CVG operation:

1. Rate mode or closed loop mode [2, 4-6], where a stable amplitude primary standing wave excited in a vibrating structure at one of its resonant frequencies is retained in the vicinity of the drive electrode by the control forces. Gyro rotation originates Coriolis force exciting a secondary standing wave that is compensated for by applying the control forces to keep the standing wave in the initial position in the vicinity of the drive electrode. Amplitude of the control signal that compensates for the Coriolis force is proportional to angle rate.
2. Rate-integrating mode or whole angle mode [4, 5, 8], where under gyro rotation, Coriolis force is not compensated for and causes a standing wave rotation providing transformation of vibration energy from primary to secondary modes and vice versa. Quadrature signal is the only one that is compensated for to reduce CVG errors [4]. In this case, gyro rotation angle in inertial space is proportional to standing wave rotation angle caused by Coriolis forces.
3. Comparatively recent investigations [9] made in Ukraine resulted in the creation of a third, differential, mode of CVG operation which complements the first two modes having additional capabilities for suppression of external disturbances like shock, vibration [10], sound and magnetic fields [11]. In the diffrential mode of operation a standing wave is retained in between the electrodes, forming two measuring channels with opposite signs of the angle rate. The difference of the two channel signals increases signal-to-noise ratio and decreases external disterbances, which appear on both channels with the same signs.

The first, rate, mode of CVG operation is most popular one because of lower influence of manufacturing imperfections, lower noise when measuring small angle rate and it has an acceptable bandwidth for most applications. The second, rate-integrating (whole angle), mode can have extremely high dynamic range, high bandwidth and very stable scale factor, but it has higher sensitivity to manufacturing imperfections. The third one has higher resistance to external disturbances.

CVGs defer from other gyroscope technologies by that all practically interesting, which we are numbered here as the first, second and third modes of operation can be implemented in a single multi-mode vibratory gyroscope with automatic switching from one mode to other [3]. The latter gives undeniable advantages of CVGs over competitive technologies like ring laser and fiber optic gyros, in terms of dynamic range and bandwidth in measuring high angle rate, lower noise in measuring small angle rate, higher resistance to external disturbances and reliability [12].

For example, under measuring small angle rate it is advisable to operate in the rate mode, since the measurement errors are mainly determined by noise and bias drift which can be lower, than that of for rate-integrating modes of operation. Under measuring of high angle rate (more than 500 deg/s) or higher, it is advisable to operate in the second, rate-integrating, mode of operation since the measurement errors are mainly determined by multiplicative error $\Delta\Omega$ caused by scale factor uncertainty (ΔSF), $\Delta\Omega=\Delta SF*\Omega$. Scale factor for rate-integrating mode of operation is a stable constant (Bryan coefficient). It can reach 35 ppm and its dynamic range is up to 7×10^3 deg/s and more for even low-cost gyros [15].

When gyro is operating under high external disturbances (shocks, vibrations, magnetic and sound fields or others), it is advisable to operate in the third (differential) mode of operation, since this mode of operation for single-mass CVG has high disturbance rejection factor [10].

No one of the gyros, existing in the modern market, has so high “versatility” during measuring angle rate in changing environment like CVGs.

This paper presents modeling results on rotation angle measurement of low-cost and low Q-factor CVGs operating in whole angle mode using virtual rotation and correction of periodic drift caused by a damping mismatch and a residual of frequency mismatch.

2. Whole-angle mode principle of operation

CVGs principle of operation in whole angle mode or rate-integrating mode will be considered here on the example of ring-like resonators, i.e. hemispherical, cylindrical, ring, toroidal and others which are bodies of rotation. Let’s consider a ring-like resonator that has eight electrodes located around

resonator circumferential coordinate at the equal angles of 45 deg to each other. Diametrically opposite electrodes are short-circuited as depicted by dashed lines in figure 1. In such a resonator is excited a standing wave on the second resonant mode (n=2), ω_r. It is a primary vibration. A standing wave on n=2 mode is characterized by four antinodes and four nodes with maximum and minimum vibration amplitudes, respectively. In absence of an angle rate around a CVG sensitivity axis, which is perpendicular to a ring's plane, the nodes and antinodes are located in the vicinity of the corresponding X_{drive}, X_{sense} and Y_{drive}, Y_{sense} electrodes. When the ring is rotating around sensitivity axis, their appear the Coriolis forces F_c. The resultant Coriolis force excites a secondary standing wave. Superposition of the primary and secondary standing waves results in turn of the standing wave through the angle proportional to CVG rotation angle in inertial space. In this case, a full vibration energy is dividing between primary and secondary standing waves.

As time progress, under a standing wave rotation, a vibration energy is fully transferred from primary wave to secondary one and vice versa. A standing wave rotation angle θ is connected to the CVG rotation angle as follows:

$$\theta(t) = -k\alpha(t); \alpha(t) = \int_0^t \Omega(\tau)d\tau\ , \tag{1}$$

where θ(t) is a standing wave rotation angle relative to CVG casing, α(t) is a CVG rotation angle relative to inertial space (far distant stars), k is an angle gain coefficient or Bryan coefficient, which is a CVG scale factor operating in whole angle mode.

Resonator elementary mass point motion trajectory in general case is an ellipse shown in figure 2. Ellipse parameters are designated as follows: a is a vibration amplitude, q is a quadrature amplitude caused by resonator's imperfection, ω_r is a resonant frequency, ϕ' is a vibration phase, θ is a standing wave angular position relative to X axis (drive electrode). Parameters a, q, ω_r, ϕ' and θ are called pendulum variables.

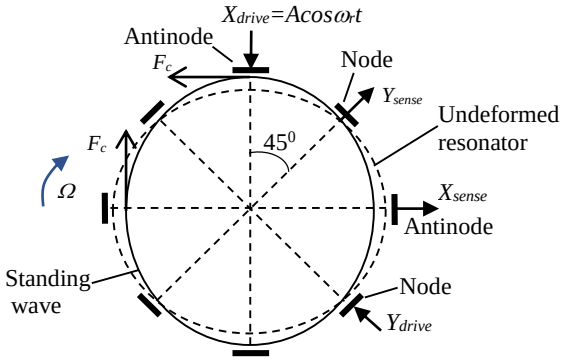

Figure 1. A standing wave in a ring-like resonator

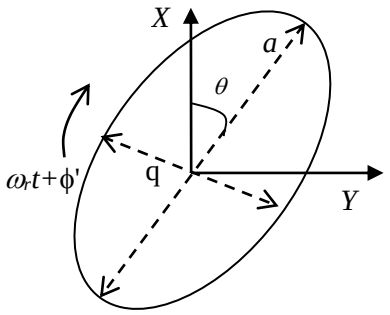

Figure 2. Mass elements motion trajectory in rate-integrating CVG

The aim of a CVG control system in rate-integrating mode of operation is to keep the pendulum variables in process of operation at the following values [14]:

$$q=0,\ a=const,\ \phi'=0. \tag{3}$$

The first equality means that mass elements trajectory must be reduced to straight line. The second one means that vibration amplitude a should be stabilized. This can be made through the vibration energy E stabilization:

$$E = A_x^2 + A_y^2 = a^2, \tag{4}$$

where A_x and A_y are vibration amplitude components along X and Y coordinate axes.

The third equality of (3) means that the vibration phase should be locked with the phase of the reference phase generator.

3. Whole-angle mode main errors

The most significant effect on a CVG errors has the fourth harmonic in Fourier expansion of the mass distribution along circumferential coordinate of a resonator, due to the differences in the ring's thickness. As a result of such a defect, the natural frequency of a resonator is split into two frequencies - maximum frequency and minimum one, which are the two principal axes of resonator's stiffness located under angle of 45^0 to each other for the second mode of vibration [15]. They are two natural frequencies of the same mode of vibration. The difference between these two natural frequencies is called frequency mismatch $\Delta\omega$:

$$\Delta\omega = \omega_2 - \omega_1, \tag{5}$$

where ω_1 is a minimum resonant frequency, and ω_2 is a maximum resonant frequency.

The fourth harmonic of the mass distribution along the circumferential coordinate of the resonator gives the following values of frequency mismatch:

$$\Delta\omega = \frac{1}{2}\varepsilon_4\omega_r, \tag{6}$$

where ε_4 is a relative value of a mass defect ($\Delta m/m$) on the fourth harmonic. These two axes are called the principal stiffness axes of a resonator.

Due to this imperfection a quadrature component of the secondary wave is created, which oscillates with the quadrature phase with respect to the primary wave, i.e. at a phase angle of 90^0. In this case, a so-called standing wave drift is appeared. The drift rate is determined by the following expression [15]:

$$\dot{\theta} = \frac{1}{8}(\Delta\omega)^2 t \sin 4\varphi_0\ , \tag{7}$$

where φ_0 is an angle between the direction of oscillation and one of the normal (principal) axes of a resonator (for example, the axis with the minimum oscillation frequency).

Another important source of CVG drift is the uneven distribution of vibration damping sources in the resonator (due to the heterogeneity of its material). As in the case of variation in the thickness of the shell, which leads to frequency mismatch, the fourth harmonic of the damping sources distribution along the circumferential coordinate, produces an effect resulting in a CVG bias drift.

Figure 3 shows a graph of a standing wave drift in dependence on its angular position in the circumferential coordinate θ. This is a sinusoidal curve with a peak value that is proportional to the inverse time constants difference:

$$\Delta\left(\frac{1}{\tau}\right) = \frac{1}{\tau_1} - \frac{1}{\tau_2} \approx \frac{\Delta Q}{Q}\frac{1}{\tau}, \tag{8}$$

where τ_1 and τ_2 are minimum and maximum resonator time constants, defined as a free oscillation amplitude damping time by $e \approx 2.7$ times, ΔQ is a Q-factor mismatch. This systematic drift is usually called as a case-oriented or angle dependent drift.

This drift is a function of very important resonator's error parameter Q-factor mismatch. A Q-factor mismatch is a function of many design parameters, resonator's material parameters, its manufacturing and assembly errors.

When CVG is operating in rate-integrating mode, residual (after balancing procedure) Q-factor mismatch results in a dead zone for small angle rate, because of primary and secondary modes synchronization (by analogy with ring laser gyro). A dead zone threshold Ω_{thr} is determined by the following expression [1]:

$$\Omega_{thr} \approx \frac{1}{2k}\left|\Delta\left(\frac{1}{\tau}\right)\right| + \frac{1}{k}\frac{q}{a}|\Delta\omega|\ , \tag{9}$$

where q is a quadrature amplitude and a is a vibration amplitude.

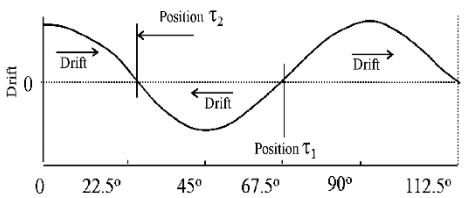

Figure 3. A case-oriented drift.

As a rule, Δω is close to zero after balancing procedure and, in addition, it is compensated by negative feedback loop during CVG operation. Thus, dead zone threshold is, in the main, determined by the first summand of expression (9), which is proportional to Q-factor mismatch ΔQ. This error cannot be compensated by negative feedback loop, because it has the same frequency and phase as an angle rate.

4. CVG whole-angle mode Simulink model

In order to model vibratory gyro, first of all sensing element dynamic equations with errors resulting from manufacturing imperfections, described above, should be accepted. There are well-known dynamic equations of two-dimensional pendulum [14] that fit for this aim:

$$\ddot{x} + d_{xx}\dot{x} + k_{xx}x + k_{xy}y = \left(2k\Omega - d_{xy}\right)\dot{y} + f_x;$$
$$\ddot{y} + d_{yy}\dot{y} + k_{xy}x + k_{yy}y = \left(-2k\Omega - d_{xy}\right)\dot{x} + f_y; \quad (10)$$

$$d_{xx} = {}^{2}/_{\tau} + \Delta\left({}^{1}/_{\tau}\right)\cos 2(\theta - \theta_\tau);\ \Delta\left(\frac{1}{\tau}\right) = {}^{1}/_{\tau_1} - {}^{1}/_{\tau_2};\ {}^{2}/_{\tau} = {}^{1}/_{\tau_1} + {}^{1}/_{\tau_2};$$
$$d_{xy} = \Delta\left(\frac{1}{\tau}\right)\sin 2(\theta - \theta_\tau);\ d_{yy} = {}^{2}/_{\tau} - \Delta\left({}^{1}/_{\tau}\right)\cos 2(\theta - \theta_\tau);$$
$$k_{xx} = \omega_1^2 - \omega\Delta\omega\cos 2(\theta - \theta_\omega);\quad k_{yy} = \omega_2^2 - \omega\Delta\omega\cos 2(\theta - \theta_\omega)$$
$$\omega\Delta\omega = (\omega_1^2 - \omega_2^2)/2; k_{xy} = \omega\Delta\omega\sin 2\,(\theta - \theta_\omega);$$

In these equations k, τ_1, τ_2, ω_1 and ω_2 have been described above, d_{xx} is the X axis damping coefficient, d_{xy} is a damping cross-coupling coefficient, k_{xx} is a normalized by mass resonator rigidity along the X axis, k_{xy} is a rigidity cross-coupling coefficient, d_{yy} is the Y axis damping coefficient, k_{yy} is a normalized by mass resonator rigidity along the Y axis, f_x, f_y are normalized by mass control signals, θ_ω is an angle between minimum frequency axis and standing wave (antinode) axis, θ_τ is an angle between minimum damping axis and standing wave axis.

It should be noted that sensing element with short-circuited diametrically opposite electrodes presents a plant with two inputs (drive electrodes X_{in} and Y_{in}) and two outputs (sense electrodes X_{out} and Y_{out}). Inputs and outputs are amplitude-modulated signals, where carrier is a resonant frequency and envelopes are corresponding standing wave control parameters.

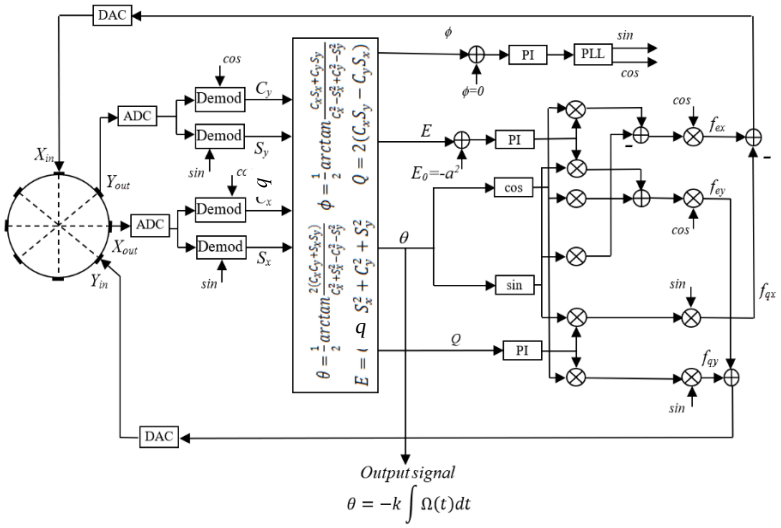

Figure 4. CVG control system block diagram operating in the whole angle mode

CVG control system block diagram is presented in figure 4. The standing wave is excited at the resonant frequency ω_r of the second mode of a ring vibration. A primary wave control is based on two subsystems: phase lock loop (PLL) and automatic gain control (AGC). These two subsystems generate a drive signal X_{in} with a proper amplitude, frequency and phase to sustain primary vibration in

changing environmental conditions. PLL provides resonant frequency tracking when it changes and AGC keeps the primary vibration amplitude at the constant desired amplitude a. A resonator response X_{out} to a drive signal X_{in} contains an error signal, which results in a vibration phase $\phi' \neq 0$. This means that excitation does not occur at resonant frequency. In this case PI controller sends to PLL a signal that induces an excitation frequency change in order to drive ϕ' to null.

At a gyro rotation there appears a signal at Y_{out} electrode from secondary vibration caused by Coriolis force together with an error signal, due to resonator imperfection, which is called quadrature, q. These two signal components are separated by demodulation processes using reference signals, $\sin\omega_r t$ and $\cos\omega_r t$, generated by PLL. Quadrature signal is driven to null by PI controller of quadrature loop. Coriolis force causes rotation of a standing wave. A standing wave rotation angle θ is computed by the demodulated signals C_x, C_y, S_x, S_y as follows:

$$\theta = \frac{1}{2}\arctan\frac{2(C_xC_y+S_xS_y)}{C_x^2+S_x^2-C_y^2-S_y^2} \qquad (11)$$

CVG whole angle mode Simulink model is based on a two-dimensional pendulum model of resonator presented by equations (10) and a control system model presented in figure 4 block diagram.

A full CVG whole angle mode Simulink model is presented in figure 5. It consists of an angle rate generator, sensing element that has four inputs, apart from drive forces f_x and f_y, it has input from angle rate generator and input signal of changing wave angle θ from wave control unit. Demodulation unit, which has five inputs: reference signals $\sin\omega_r t$ and $\cos\omega_r t$ from PLL output of control unit used to demodulate X_{sense} and Y_{sense} (X_{out} and Y_{out} in figure 4) signals coming from sensing element and inactive input assigned for noise input (as an option). Outputs of demodulation unit are the four demodulated signals C_x, C_y, S_x, S_y. Wave parameters calculation unit transforms the demodulated signals into pendulum variables a, q, ω_r, ϕ' and θ (see (11)) using the following expressions:

$$a^2 = E = C_x^2 + S_x^2 + C_y^2 + S_y^2;\ q = 2\left(C_xS_y - C_yS_x\right);$$

$$\phi' = \frac{1}{2}\arctan\frac{2(C_xC_y+S_xS_y)}{C_x^2-S_x^2+C_y^2-S_y^2}. \qquad (12)$$

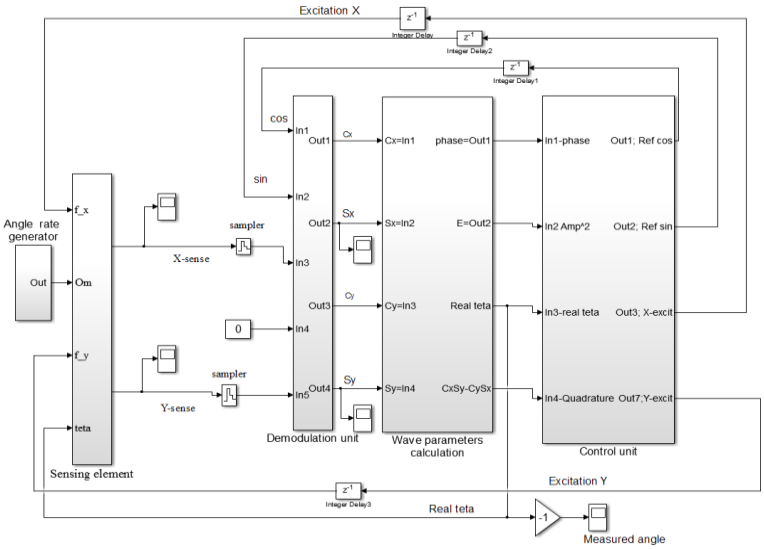

Figure 5. Full CVG Simulink model operating in the whole angle mode

Resonant frequency ω_r can be estimated by the PLL output using one of the different known algorithms [16]. This unit is calculating signal θ by expression (11) and sends it to the sensing element and to a CVG output.

Control unit has four inputs for the pendulum variables a, q, ϕ' and θ and four outputs: f_x, f_y to

sustain vibration and drive to null quadrature signal q and reference signals $\sin\omega_r t$ and $\cos\omega_r t$ for demodulation.

5. Modeling Results

Before starting modeling the gyro scale factor (*SF*) or angular gain coefficient *k* should be determined in order to convert modeling output into an angle measure. Standard methodic is used here which consists of rotation clock-wise and counter clock-wise through the equal angles α excluding transients from the measurement data and using the following expression to calculate *SF*:

$$SF = k = \frac{\theta^+ - \theta^-}{2\alpha}\ , \quad (13)$$

where θ^+ and θ^- are standing wave rotation angles clock-wise and counter clock-wise.

The following sensing element parameters have been set in the model: Q-factor=22000, ΔQ=1000, ω_r=4 kHz, $\Delta\omega$=0.188 rad/s=0.03 Hz, θ_τ=10 deg, θ_ω=5 deg.

To overcome dead zone for low Q-factor CVG the virtual rotation of the standing wave has been applied with the angle rate equal to Ω_{virt}=378.830855 deg/s.

The virtual rotation angle is automatically subtracted from the sum of virtual and actual rotation angle to obtain actual rotation angle only. Figure 6 shows a graph of such measurements. The angle rate value has been set equal to 200 deg/s. In order to exclude transients from the measurement data of the first second after starting and after switching from plus to minus rotation did not take into account.

Thus, actual rotation angle to and from has been ±800 deg, and measurement angles are:

θ^+=θ(5)-θ(1) =108.114365 deg;
θ^-=θ(10)-θ(6) =-108.161009 deg;
k= (108.114365+108.161009)/1600= 0.13517210875.

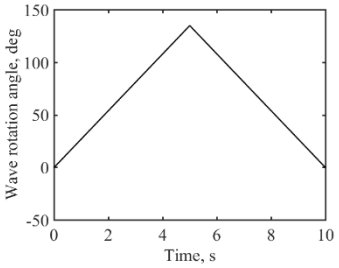

Figure 6. CVG whole angle mode SF measurement

Knowing *k* the threshold dead zone angle rate Ω_{thr} can be calculated by the expression (9) taking into account approximation (8) and neglecting the second term of the sum, one can obtain:

$$\Omega_{thr} \approx \frac{1}{2k}\left|\Delta\left(\frac{1}{\tau}\right)\right| \approx \frac{1}{2k}\frac{1}{\tau}\frac{\Delta Q}{Q} = \frac{1000}{2*0.13517*1.75*22000} \approx 0.096 \text{ Hz} \approx 34.5 \text{ deg/s} \qquad (14)$$

Using virtual rotation small angle rate can be measured, which is much less, than threshold Ω_{thr}.

Figure 7 shows measurement angle, when angle rate is 0.5 deg/s. Actual rotation is started after 1 s of virtual rotation. The waveness of the stright line of figure 7 shows angle dependent (case-oriented) periodic drift due to Q-factor mismatch. Angle of the 2 deg measurement error is 0.0087 deg.

Figure 8 shows extracted from the measurement a case-oriented periodic drift. As can be seen

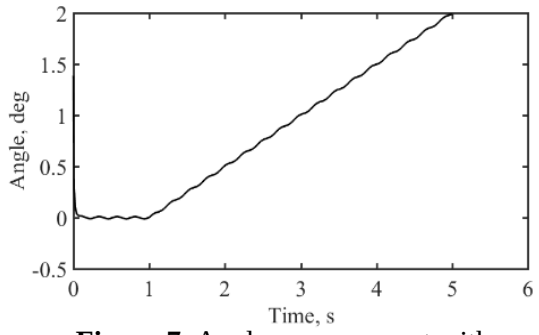

Figure 7. Angle measurement with low Q-factor CVG

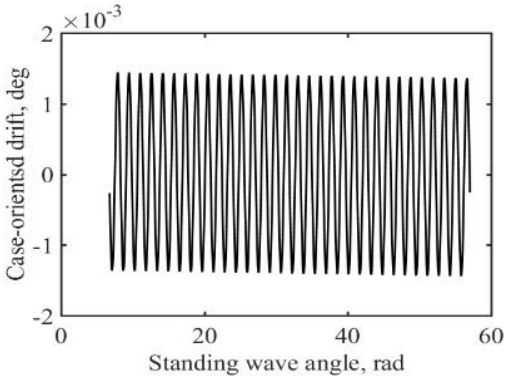

Figure 8. Angle dependent periodic drift

from figure 8, amplitude of periodic drift is less, than angle error obtained. This means that there are other errors which increase the resulting angle measurement error, such as, for example, residual error from subtraction of virtual rotation angle, small transient after starting actual rotation etc.

This angle dependent drift has four periods for one revolution of a wave around resonator circumferential coordinate. This error can be modeled and extracted from the measurements. Angle dependent periodic drift model, for resonator parameters indicated above, is approximated by the following expression obtained by least square approximation of the measurement data:

$$d(t) = 0.001402852\sin(4\theta(t) + 1.29725) \quad (15)$$

Figure 9 shows graphs of the two measurements without and with correction of the modeled error $d(t)$. After correction of angle dependent drift angle measurement error reduces to 0.0012 deg.

Figure 10 shows the two graphs of angle measurements without correction of the periodic drift under a periodic angle rate $\Omega=3\sin(2*\pi*5*t)$ and the true angle imposed on it.

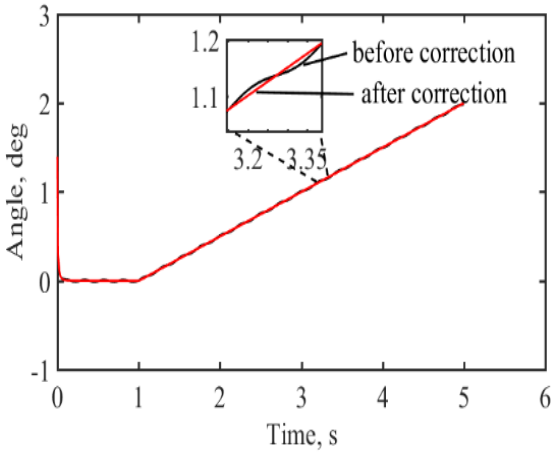

Figure 9. Periodic drift correction

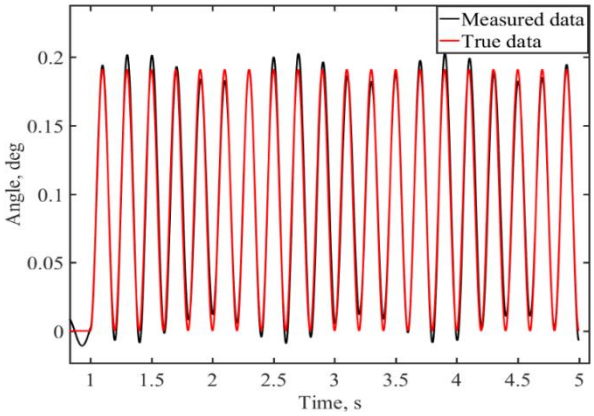

Figure 10. Angle measurement of a periodic angle rate without correction

Angle measurement errors under periodic angle rate with correction by the model presented in (15) and without it are presented in figure 11. It shows that correction of the periodic drift reduces measurement error about two times.

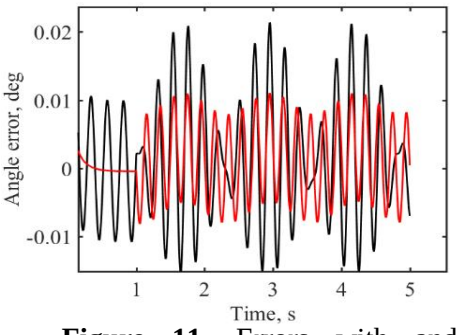

Figure 11. Errors with and without periodic drift correction

Conclusion

The scale factor of the CVG operating in a whole angle mode is a stable constant that depends on the vibration mode and the geometry of the resonator.

The angle measurement error by the rate-integrating (whole angle mode) CVG is a periodic function of the standing wave angle, the amplitude of which is proportional to the Q-factor and frequency mismatches. Under balancing frequency mismatch to small values, the amplitude of the error is proportional to the Q-factor mismatch and inverse proportional to Q-factor.

The rate-integrating CVG has a zone of insensitivity to a small angle rate or a dead zone. The dead zone threshold is proportional to Q-factor mismatch and inverse proportional to Q-factor.

Measurement of angles at small angle rates, for rate-integrating gyroscopes with a low Q-factor resonator is possible by creating a virtual rotation of the standing wave, which simulates the virtual angle rate significantly exceeding the threshold value of the dead zone angle rate.

The small angles measurement error mainly depends on the amplitude of the angle dependent periodic error, so called case-oriented drift.

A standing wave angle dependent periodic error can be corrected, for example, by building a mathematical model of this error, thus increasing angle measurement accuracy.

References

[1] Prikhodko I P, Zotov S A, Trusov A A and Shkel A M 2012 Foucault pendulum on a chip: Rate integrating silicon MEMS gyroscope. *Sensors and Actuators A: Physical* 177 pp 67-78 doi:10.1016/j.sna.2012.01.029.

[2] Lynch D D and Matthews A 1996 Dual Mode Hemispherical Resonator Gyro Operating Characteristics. *3-rd S. Petersburg Int. Conf. on Integrated Navigation Systems.* part 1 pp 37-44

[3] Chikovani V V and Tsiruk H V 2015 Differential Mode Of Operation For Multimode Vibratory Gyroscope. *IEEE Proc. Intern. Conf. on Actual Problem of Unmanned Aerial vehicles Development (APUAVD),* NAU, Kyiv, Ukraine. Oct. 13-15 pp 87-90

[4] Cho J Y 2012 High-Performance Micromachined Vibratory Rate- And Rate- Integrating Gyroscopes. Ph.D. Dissertation, Michigan University p 293

[5] Woo J-K, Cho J Y, Boyd Ch and Najafi Kh 2014 Whole-Angle-Mode Micromachined Fused-Silica Birdbath Resonator Gyroscope. (Wa-Brg), *IEEE MEMS Conf.,* San Francisco, CA, USA, January 26-30

[6] Zhong Su, Ning Liu, Qing Li, Mengyin Fu, Hong Liu and Junfang Fan 2014 Research on the Signal Process of a Bell-Shaped Vibratory Angular Rate Gyro. *Sensors.* 14 5254-5277 doi: 10.3390/s140305254

[7] Gallacher B, Hu Zh and Bowles S 2015 Full control and compensation scheme for a rate-integrating MEMS gyroscope. *13th Int. Conf. on Dynamical Systems - Theory And Applications*, Lodz, Poland. paper id: ENG267 Dec. 7-10

[8] Gregory J A 2012 Characterization Control and Compensation of MEMS Rate and Rate-Integrating Gyroscopes. Ph.D. Dissertation, Michigan University, p 198

[9] Chikovani V V and Suschenko O A 2014 Differential mode of operation for ring-like resonator CVG. *IEEE Proc. Intern. Conf. on Electronics and Nanotechnology*, Kyiv, Ukraine, 15-18 April, pp 451-455

[10] Valerii V Chikovani, Olha A Sushchenko and Hanna V Tsiruk 2017 External Disturbances Rejection by Differential Single-Mass Vibratory Gyroscope. Acta Polytechnica Hungarica, Vol 14 #3 pp 251-270

[11] Chikovani Valeriy and Sushchenko Olha 2019 Self-Compensation for Disturbances in Differential Vibratory Gyroscope for Space Navigation. *Hindawi, International Journal of Aerospace Engineering.* v Article ID 5234061, 9 pages, https://doi.org/10.1155/2019/5234061

[12] David M Rozelle: Hemispherical Resonator Gyro: From Wineglass to the Planets, http://www.northropgrumman.com/capabilities/hrg/documents/hrg.pdf

[13] Jeanroy A, Featonby P and Caron J-M 2003 Low-Cost Miniature and Accurate Sensors for Tactical Applications. 10-th S. Petersburg Int. Conf. on Integrated Navigation Systems, pp 286-293

[14] Lynch D D 2004 “Coriolis Vibratory Gyroscope, IEEE Standard Specification Format Guide and Test Procedure for Coriolis Vibratory Gyros”// IEEE std.1431TM, Annex B pp 56-66 Dec.

[15] Matveev V A, Lunin B S and Basarab M A 2008 Navigation Systems Based on Solid-State Wave Gyroscopes” (Moscow: Fizmatlit) p 239

[16] Kootsookos P J 1999 Review of the Frequency Estimation and Tracking Problems. – Report for Robust and Adaptive Systems, DSTO, Salisbury Site